Synthesis, crystal structures and magnetic properties of the oxalate-bridged single $Cu^{II}Cu^{II}$ and cocrystallized $Cu^{II}Zn^{II}$ systems. Three species (CuCu, CuZn, ZnZn) in the crystalline lattice

Marijana Jurić,[a]***** **Damir Pajić,**[b] **Dijana Žilić,**[a] **Boris Rakvin,**[a] **Dalibor Milić,**[c] **and Pavica Planinić**[a]*****

[a] *Ruđer Bošković Institute, Bijenička cesta 54, 10000 Zagreb, Croatia.*

[b] *Department of Physics, Faculty of Science, University of Zagreb, Bijenička cesta 32, 10000 Zagreb, Croatia.*

[c] *Department of Chemistry, Faculty of Science, University of Zagreb, Horvatovac 102a, 10000 Zagreb, Croatia; Present address: Paul Scherrer Institut, 5232 Villigen PSI, Switzerland*

Marijana Jurić

Ruđer Bošković Institute, Bijenička cesta 54, 10000 Zagreb, Croatia

Tel.: +385 1 4561-189

Fax: +385 1 4680-098

E-mail: Marijana.Juric@irb.hr

Pavica Planinić

Ruđer Bošković Institute, Bijenička cesta 54, 10000 Zagreb, Croatia

Tel.: +385 1 4561-189

Fax: +385 1 4680-098

E-mail: planinic@irb.hr

ABSTRACT

Two novel oxalate-bridged species: homometallic $Cu^{II}Cu^{II}$, $[\{Cu(bpy)Cl\}_2(\mu\text{-}C_2O_4)]$ (**1**) and heterometallic $Cu^{II}Zn^{II}$, $[CuZn\{(bpy)Cl\}_2(\mu\text{-}C_2O_4)]$ (**2**) (bpy = 2,2'-bipyridine), were synthesized and characterized by elemental analyses, IR and EPR spectroscopy, magnetic susceptibility measurements and single-crystal X-ray diffraction studies. The compounds crystallise in the same, triclinic $P\overline{1}$ space group. Their crystal structures consist of the binuclear entities $[M(bpy)Cl(\mu\text{-}C_2O_4)M(bpy)Cl]$ [M = Cu^{2+} (**1**); M = Cu^{2+} and/or Zn^{2+} (**2**)] linked by the intermolecular π···π stacking interactions. Highly unusual, compound **2** is a cocrystallized system containing three types of mutually analogous entities: $[Cu(bpy)Cl(\mu\text{-}C_2O_4)Cu(bpy)Cl]$ (**CuCu**; the same unit as in **1**), $[Cu(bpy)Cl(\mu\text{-}C_2O_4)Zn(bpy)Cl]$ (**CuZn**) and $[Zn(bpy)Cl(\mu\text{-}C_2O_4)Zn(bpy)Cl]$ (**ZnZn**), randomly distributed throughout the crystalline lattice in the molar ratio near to 1 : 2 : 1, respectively. Each metal atom in both **1** and **2** displays a square-pyramidal coordination involving two N atoms from the coordinated 2,2'-bipyridine ligand and two O atoms from the bridging oxalate group in the basal plane, and one chlorine atom in the apical position. Magnetization measurements, supported also by the EPR study, reveal a strong antiferromagnetic exchange interaction (J = –295(2) and –294(2) cm^{-1}, for **1** and **2**, respectively; $\mathbf{H} = -J\mathbf{S_1}\cdot\mathbf{S_2}$) between two copper(II) ions through the oxalate bridge.

Keywords: Binuclear copper compound; Binuclear zinc compound; Oxalate bridges; Homo- and heterometallic; Magnetic properties

1. Introduction

In the last few decades, the chemistry of oxalate-containing complexes has been an active area of research, with the interest arising from various structural features of these compounds [1] and in particular from their applications in the fields such as crystal engineering [2] and molecular magnetism [3]. The rich binding facilities of the oxalate $C_2O_4^{2-}$ anion, and its ability of mediating magnetic exchange interaction between the paramagnetic metal centres are responsible for the existence of a huge number of oxalate-bridged transition metal species, of different nuclearity and dimensionality [1c], which also exert a range of distinct magnetic properties. The introduction of organic ligands like 2,2'-bipyridine and related species, into the metal-oxalate systems further stabilizes their solid-state structures. The non-covalent interactions such as $\pi \cdots \pi$ stacking and hydrogen bonding may adjust the dimensionality and lead to new topologies and desired functions of these metallosupramolecular assemblies [4].

Copper is one of the most important transition metals, especially because of its biological relevance [5], but also with respect to its magnetochemistry [3a]. The rich stereochemistry of copper(II), based on its multiple coordination modes, gives rise to an enormous structural diversity in the copper(II) coordination chemistry [1c]. A special emphasis is given to the binuclear oxalate-bridged copper(II) complexes [6,7] as ideal candidates for the systematic investigations of correlations between structural and magnetic properties, from both experimental and theoretical viewpoints.

The zinc(II) μ-oxalate complexes have been paid extensive attentions for their appealing optic properties and structural topology [8,9]. A particularly great importance of zinc complexes is found also in the field of synthetic and biological chemistry, due to the role this element plays in biological systems – fulfilling structural and different catalytic functions in a great number of enzymes [10].

Binuclear homo- and heterometallic complexes are often used as model compounds in order to simulate characteristic properties of the active sites in different metalloenzymes [11]. Thus, a number of binuclear [Cu,Cu] and [Cu,Zn] species have been prepared in order to mimic structural and/or functional properties of the [Cu,Zn] superoxide dismutase (SOD), i.e. of the enzyme that transforms the highly reactive superoxide radical ion to molecular oxygen and hydrogen peroxide. It is to be noted that the structural and chemical composition of the surrounding active sites in metalloenzymes can modulate their function. Therefore, to establish the individual roles of the two metal centres, it is necessary to know their structural characteristics. Despite the fact that a significant number of [Cu,Zn] complexes have been

prepared [12–17], only a few of them – mostly those with the macrocyclic ligands – were structurally characterized [11b,16,18].

As a continuation of our magneto-structural studies concerning the polynuclear transition-metal complexes, herein we report the synthesis, crystal structures and magnetic properties of two new oxalate-bridged compounds: homometallic $Cu^{II}Cu^{II}$, $[\{Cu(bpy)Cl\}_2(\mu\text{-}C_2O_4)]$ (**1**) and heterometallic $Cu^{II}Zn^{II}$, $[CuZn\{(bpy)Cl\}_2(\mu\text{-}C_2O_4)]$ (**2**) (bpy = 2,2'-bipyridine).

A recent literature search revealed the existence of only a few other complexes having the coplanar $[(bpy)Cu(\mu\text{-}C_2O_4)Cu(bpy)]$ moiety with the five-coordinated metal centres. However, unlike compound **1**, the fifth apical position in most of these complexes is occupied by one H_2O molecule, while the overall charge of the species is neutralized by different counter anions [19]. A neutral binuclear complex unit, as it is the case in the here described $Cu^{II}Cu^{II}$ compound (**1**), was found merely in two more species. One of them has PF_6^- in the fifth coordination site [20a], whereas the other, of the formula $[\{Cu(bpy)Cl\}_2(\mu\text{-}C_2O_4)]\cdot H_2O$ [20b], has chlorine at the apical positions – similarly as compound **1**, but its crystal structure differs significantly from the structure of **1**. Up to now, two oxalate-bridged $Cu^{II}Zn^{II}$ complexes were reported: $[(dien)Cu(\mu\text{-}C_2O_4)Zn(dien)](BPh_4)_2$ (dien = ethylenediamine) and $[(PMDT)Cu(\mu\text{-}C_2O_4)Zn(PMDT)](BPh_4)_2\cdot 2CH_3CN$ (PMDT = pentamethyldiethylenetriamine); however, these species were investigated primarily in relation with their biological activities [17], and their crystal structures have never been determined.

It is also to be noted that the reported compounds, both **1** and **2** have been obtained following an atypical synthetic route. A particularly interesting feature of compound **2** is that its structure consists of three types of mutually analogous binuclear entities: $[Cu(bpy)Cl(\mu\text{-}C_2O_4)Cu(bpy)Cl]$ (**CuCu**), $[Cu(bpy)Cl(\mu\text{-}C_2O_4)Zn(bpy)Cl]$ (**CuZn**) and $[Zn(bpy)Cl(\mu\text{-}C_2O_4)Zn(bpy)Cl]$ (**ZnZn**), randomly distributed throughout the same crystalline lattice in the molar ratio close to 1 : 2 : 1, determined by the measurements on SQUID-magnetometer. In addition to the magnetic susceptibility and single crystal X-ray diffraction, the characterization of the novel compounds (**1** and **2**) has been accomplished by means of IR and EPR spectroscopy.

2. Experimental

2.1. Materials and physical measurements

The starting species $[Cu(bpy)_3]Cl_2\cdot 6H_2O$ was prepared according to the method described in the literature [21]. All other reagents were purchased from commercial sources, and used

without further purification. During the synthesis of compound **2** all operations were performed under a nitrogen atmosphere in a dry-box. Elemental analyses for C, H and N were carried out using a Perkin Elmer Model 2400 microanalytical analyser. Metal analysis for Cu and Zn were made on a high resolution thermal field scanning electron microscope model JEOL 7000F with EDS (Energy Dispersive X-ray Spectroscopy) system for the microanalysis INCA 350, Oxford Instruments. In addition, Cu and Zn were determined by a Varian SpectrAA 220 atomic absorption spectrometry (AAS). The amount of oxalate was obtained by titration with standard $KMnO_4$ solution. The chlorine content was determined by titration with standard $AgNO_3$ solution after decomposition of samples with KOH and H_2O_2. Infrared spectra were recorded as KBr pellets with an ABB Bomem FT model MB 102 spectrometer in the 4000–200 cm^{-1} region. Electronic spectra were measured with a Cary 50 Probe spectrophotometer.

2.2. Synthesis

2.2.1. Preparation of [{Cu(bpy)Cl}$_2$(µ-C$_2$O$_4$)] (1)

The scraping of Zn (0.196 g, 3 mmol) was dissolved in a 2 : 3 mixture (4 mL) of conc. HCl and EtOH, and an aqueous solution (4 mL) of $K_2C_2O_4 \cdot H_2O$ (0.976 g, 5.3 mmol) was added dropwise. Immediately, the reaction mixture became cloudy forming a white precipitate. The pH value of the mixture was adjusted to 1.5 with an 8M KOH aqueous solution. Then, an aqueous solution (8 mL) of $[Cu(bpy)_3]Cl_2 \cdot 6H_2O$ (0.306 g, 0.43 mmol) was added, which was followed by the formation of a blue precipitate. The day after, the precipitate was removed by filtration and the clear solution was left to evaporate at ambient conditions. The blue prismatic single crystals of **1**, formed over a period of four days, were filtered off, washed with water and briefly dried in air. Yield: 42%. Anal. Calcd. for $C_{22}H_{16}Cl_2Cu_2N_4O_4$ (Mr = 598.37): C, 44.16; H, 2.70; Cl, 11.85; N, 9.36; C_2O_4, 14.71%. Found: C, 43.98; H, 2.52; Cl, 11.96; N, 9.45; C2O4, 14.92%. IR data (KBr, cm^{-1}): 3448 (w, br), 3105 (w), 3065 (m), 3050 (m), 3020 (m), 1647 (vs), 1607 (s), 1598 (s), 1572 (w), 1563 (w), 1493 (m), 1473 (m), 1446 (m), 1433 (sh), 1351 (m), 1314 (m), 1282 (w), 1255 (w), 1229 (w), 1171 (w), 1159 (m), 1123 (w), 1110 (w), 1071 (w), 1052 (w), 1032 (m), 1019 (w), 983 (w), 976 (w), 821 (m), 796 (m), 782 (s), 757 (sh), 730 (m), 661 (w), 649 (w), 640 (w), 481 (m), 433 (w), 421 (m), 325 (m), 302 (w).

2.2.2. Preparation of [CuZn{(bpy)Cl}$_2$(µ-C$_2$O$_4$)] (2)

$NbCl_5$ (0.113 g, 0.42 mmol) was dissolved in the conc. HCl/EtOH (2 : 3) mixture (4 mL),

and then the zinc scraping (0.196 g, 3 mmol) was added for reduction. After all the amount of zinc reacted, an aqueous solution (4 mL) of $K_2C_2O_4 \cdot H_2O$ (1.013 g, 5.5 mmol) was added slowly forming a brown slurry. The pH value of the mixture was adjusted to 1.5 by a dropwise addition of an 8M KOH aqueous solution. The reaction mixture was left for 20 minutes, when the brown-coloured solution was decanted and mixed with an aqueous solution (8 mL) of $[Cu(bpy)_3]Cl_2 \cdot 6H2O$ (0.306 g, 0.43 mmol). The colour of the mixture changed from brown toward blue and soon, a blue precipitate appeared. The day after, the green plate-like single crystals of **2** formed. The crystals were collected by filtration, washed several times with mother-liquid to remove the traces of the blue powdered precipitate, and then washed with water and air dried.

Note. The above synthesis procedure, as it involves an airsensitive niobium(IV) intermediate, was performed under an inert-gas atmosphere in a dry-box.

Yield: 55 %. Anal. Calcd. for $C_{22}H_{16}Cl_2CuN_4O_4Zn$ (Mr = 600.20): C, 44.03; H, 2.69; Cl, 11.81; N, 9.33; C_2O_4, 14.66%. Found: C, 44.15; H, 2.58; Cl, 11.98; N, 9.40; C2O4, 14.85%. IR data (KBr, cm^{-1}): 3449 (w, br), 3103 (w), 3066 (m), 3048 (m), 3020 (m), 1649 (vs), 1606 (s), 1597 (s), 1572 (w), 1563 (w), 1492 (m), 1474 (m), 1447 (m), 1431 (sh), 1352 (m), 1315 (m), 1282 (w), 1255 (w), 1229 (w), 1172 (w), 1159 (m), 1123 (w), 1110 (w), 1072 (w), 1052 (w), 1033 (w), 1025 (m), 1019 (w), 983 (w), 975 (w), 822 (m), 797 (m), 781 (vs), 757 (sh), 730 (s), 660 (w), 649 (w), 640 (w), 482 (s), 432 (w), 420 (s), 325 (w), 298 (m), 305 (sh).

2.3. Single-crystal X-ray study

The X-ray data for the single crystals of **1** and **2** were collected at 110 K by ω-scans on an Oxford Diffraction Xcalibur 3 CCD diffractometer with the graphite-monochromated Mo-Kα radiation ($λ$ = 0.71073 Å). The crystallographic data are summarized in Table 1. The data reduction (including the analytical absorption correction) [22] was performed using the CrysAlis software package [23]. Solution, refinement and analysis of the structures were done using the programs integrated in the WinGX system [24]. The structures were solved by direct methods (SHELXS) [25] and refined by the full-matrix least-squares method based on F^2 against all reflections (SHELXL-97) [25]. Structure **2** manifests a static substitutional disorder involving **CuCu**, **CuZn** and **ZnZn** species in a molar ratio 1 : 2 : 1. The **CuCu** and **ZnZn** entities in **2**, the same as the binuclear entities of **1**, possess a real crystallographic inversion centre in the middle of the bridging oxalate ligand. Although the **CuZn** entities lie on the crystallographic inversion centre, they are not centrosymmetric; in this case, the crystallographic inversion centre is the consequence of two different and equally probable

CuZn molecular orientations related by the inversion symmetry. During the refinement, the assumption was taken that there is no substantial difference between the geometry around a single metal centre in the homometallic entity, **CuCu** or **ZnZn**, and the geometry around the same metal centre in the heterometallic entity **CuZn**. Therefore, the geometry around the Cu atom was modelled the same regardless the entity (homo- or heterometallic) to which it belongs. The same applies to Zn, as well, resulting in two structural models in the asymmetric unit. Each metal atom and the ligands bound to it (except for the oxalate) were modelled with a site occupancy factor of 1/2. The oxalate group was not modelled as discretely disordered; therefore, its position is the same for both metal atoms. During the refinement of compound **2**, as a substitutional static disorder was modelled, restraints were applied regarding the following: (a) the atomic displacement parameters, (b) the geometry around Cu (which was restrained to be like that in compound **1**), and (c) the geometry of pyridyl rings. All non-hydrogen atoms in both **1** and **2** were refined anisotropically, except for the atoms of the bipyridine ligand in **2** which were refined isotropically, because anisotropic refinement for these atoms did not converge. The hydrogen atoms in both structural models were treated as riding in idealized positions [d(C–H) = 0.95 Å; U_{iso}(H) = 1.2U_{eq}(C)]. Geometrical calculations were performed using PLATON [26] and the figures were made using PLATON [26] and ORTEP-3 [27].

Table 1
Crystallographic data and structure refinement for compounds **1** and **2**.

	1	2
Chemical formula	$C_{22}H_{16}Cl_2Cu_2N_4O_4$	$C_{22}H_{16}Cl_2CuN_4O_4Zn$
M_r	598.37	600.20
Crystal colour, habit	blue prism	green plate
Crystal size (mm^3)	0.18 × 0.31 × 0.50	0.09 × 0.24 × 0.27
Crystal system	triclinic	triclinic
Space group	$P\bar{1}$	$P\bar{1}$
a (Å)	8.059(3)	8.1097(5)
b (Å)	8.3121(8)	8.3404(5)
c (Å)	8.890(3)	8.8930(5)
α (°)	71.525(18)	71.524(5)
β (°)	80.86(3)	80.947(5)
γ (°)	71.423(19)	70.873(6)
V (Å^3)	534.3(3)	538.05(6)
Z	1	1
D_{calcd} (g cm^{-3})	1.860	1.852
μ(Mo-K$_\alpha$) (mm^{-1})	2.281	2.392
T_{min}/T_{max}	0.425/0.692	0.557/0.819
θ_{max} (°)	30.0	30.0
Limiting indices	$-11 \leq h \leq 10$	$-11 \leq h \leq 11$
	$-11 \leq k \leq 11$	$-11 \leq k \leq 11$

	$-12 \leq l \leq 12$	$-12 \leq l \leq 12$
Data total/unique		
Observed data [$I > 2\sigma(I)$]	8037/3095	7702/3118
R_{int}	2901	2644
Parameters/restraints	0.015	0.019
$R_1{}^{a}$, $wR_2{}^{b}$ [$I > 2\sigma(I)$]	154/0	148/70
R_1, wR_2 (all data)	0.0218, 0.0545	0.0325, 0.0735
GOF^{c}	0.0232, 0.0552	0.0419, 0.0757
Residuals (e Å^{-3})	1.094 (1.094)	1.083 (1.076)
	0.417, −0.571	0.614, −0.416

^{a} $R_1 = \sum||F_o| - |F_c||/\sum|F_o|$. ^{b} $wR_2 = [\sum w(F_o{}^2 - F_c{}^2)^2/\sum w(F_o{}^2)^2]^{1/2}$. ^{c} GOF = $[\sum w(F_o{}^2 - F_c{}^2)^2/(N_{ref} - N_{par})]^{1/2}$; the values in parentheses explicitly include the restraints applied in the refinement: GOF = $[(\sum w(F_o{}^2 - F_c{}^2)^2 + \sum w_r(P_{calc} - P_{targ})^2)/(N_{ref} + N_{restr} - N_{par})]^{1/2}$.

2.4. Magnetic studies

Magnetic measurements were carried out using a commercial SQUID magnetometer (MPMS-5, Quantum Design). Magnetization of the pulverised samples of compounds **1** and **2** was measured in the temperature range 1.8–300 K at several values of applied magnetic field. Linearity of magnetization with field was observed up to more than 1 T for several different temperatures. Moreover, the susceptibility curves $\chi(T)$ were independent on the applied magnetic field for all measured fields below 1 T and through the whole range of temperature. Therefore, the measurements performed at 1 T are fully reliable and were chosen for the analysis of temperature dependence of magnetic susceptibility $\chi(T)$ for compounds **1** and **2**.

Electron paramagnetic resonance (EPR) measurements were performed on powdered samples of compounds **1** and **2** by an Xband EPR spectrometer (Bruker Elexsys 580 FT/CW) that was equipped with a standard Oxford Instruments model DTC2 temperature controller. The measurements were obtained at the microwave frequency around 9.7 GHz with magnetic field modulation amplitude of 0.3 mT at 100 kHz. The EPR spectra were recorded in the temperature range 5–295 K.

3. Results and discussion

3.1. Synthesis and characterization

Compound **1** was obtained in the form of blue prismatic crystals from the reaction mixture containing an HCl/EtOH solution of Zn and an aqueous solution of $K_2C_2O_4 \cdot H_2O$, to which an aqueous solution of [Cu(bpy)$_3$]Cl$_2 \cdot$6H$_2$O was added. It is to be noted that compound **1** forms only in the case when zinc is present in the reaction mixture; otherwise, the known polymeric species {[Cu(bpy)(μ-C$_2$O$_4$)]·2H$_2$O}$_n$ occurs [28]. In the synthesis of compound **2**, the starting

reaction mixture contained a niobium(IV) species (resulted from the reduction of $NbCl_5$ by Zn in an HCl/EtOH medium), to which an aqueous solution of $K_2C_2O_4 \cdot H_2O$ was added, forming a brown slurry. To the clear (decanted) brown-coloured solution (with a niobium(IV) intermediate, whose presence was confirmed by UV/Vis spectroscopy [29], Fig. S1 in the Supporting information), an aqueous solution of $[Cu(bpy)_3]Cl_2 \cdot 6H_2O$ was added, giving rise to the green plate-like single crystals of **2**. In both cases the pH values of the mixtures were strongly controlled and adjusted to pH = 1.5 before adding $[Cu(bpy)_3]Cl_2 \cdot 6H_2O$. The EDS analysis on a few single crystals showed that the blue prismatic crystals of **1** contain Cu as the only metal element, and that the green plate-like crystals of **2** contain both Cu and Zn in the atomic ratio close to 1. Also, the elemental analysis, made by the AAS method, confirmed that compound **2** contains Cu and Zn in a molar ratio of 1 : 1.

The described synthetic procedures evolved from our intention to introduce a paramagnetic Nb species in the reactions with other transition metal ions, which would lead to heterometallic $M^{II}Nb^{IV}$ compounds with more interesting magnetic properties. Specifically, we meant to extend our studies from the $[NbO(C_2O_4)_3]^{3-}$ building block chemistry [30] to the use of $[Nb(C_2O_4)_4]^{4-}$ as a new building unit [29,31]. While the research related to the $Cu^{II}Nb^{IV}$ oxalate-bridged species is still in progress, the procedure described above resulted in compound **2** ($Cu^{II}Zn^{II}$). Obviously, the presence of a kind of niobium(IV) species in the reaction mixture has a crucial role on the inclusion of Zn into the oxalate-bridged system of **2**. On the other hand, our efforts to prepare the $Cu^{II}Zn^{II}$ compound without the use of the niobium(IV) intermediate resulted in the blue crystals of compound **1** ($Cu^{II}Cu^{II}$).

3.2. Crystal structure of 1

The crystal structure of compound **1** consists of the centrosymmetric binuclear entities $[Cu(bpy)Cl(\mu\text{-}C_2O_4)Cu(bpy)Cl]$ linked by the intermolecular $\pi \cdots \pi$ stacking interactions of the aromatic rings and weak C–H$\cdots$Cl hydrogen bonds. The molecular structure of the binuclear unit of **1** is shown in Fig. 1, and the selected geometric parameters are given in Table 2. The oxalate group, with a crystallographic inversion centre lying in the middle of its C–C bond, bridges two Cu atoms in the usual bis(bidentate) fashion. The Cu atom displays a square-pyramidal CuN_2O_2Cl coordination, involving two N atoms from the 2,2'-bipyridine ligand and two O atoms from the bridging oxalate group in the basal plane, together with a chlorine atom in the apical position. The metal atom is 0.39642(15) Å above the basal plane of the pyramid. The Cu–N and Cu–O distances average 1.9843 and 2.0074 Å, respectively (Table 2) and are in good agreement with the corresponding bond lengths found in related binuclear oxalate-

bridged copper(II) species [19,20,32]. The value of the Cu–Cl bond length [2.3869(10) Å] in **1** is somewhat smaller than the one [2.448(3) Å] found for the corresponding bond in the similar copper(II) compound [{Cu(bpy)Cl}$_2$(μ-C$_2$O$_4$)]·H$_2$O [20b], but is greater than the value [2.2629(9) Å] for the analogous bond in [{Cu(phen)Cl}$_2$(μ-C$_2$O$_4$)] (phen = 1,10-phenanthroline) [6f]; neither of these two complexes is isostructural with **1**. The two axial Cl atoms in the binuclear unit of **1** are *anti* to each other, as are also in [{Cu(phen)Cl}$_2$(μ-C$_2$O$_4$)] [6f], whereas in [{Cu(bpy)Cl}$_2$(μ-C$_2$O$_4$)]·H$_2$O [20b] the Cl atoms are *syn* to each other. The Cu···Cu^i [(i) = 1 – x, 1 – y, 1 – z] distance across the bridging oxalate group is 5.227(2) Å, which is slightly (on average by less than 0.1 Å) longer than the corresponding distances found in several other symmetric binuclear copper(II) oxalate-bridged complexes [7,19c,20a,32a]. It is interesting to note that the smallest intermetal distance in **1** [5.0967(19) Å] is the one between Cu and Cu^{iii} [(iii) = –x, 1 – y, 1 – z] from a neighbouring unit.

The centrosymmetric binuclear entities, [Cu(bpy)Cl(μ-C$_2$O$_4$)Cu(bpy)Cl], are connected by the intermolecular π···π stacking interactions through the aromatic rings of the 2,2'-bipyridine ligand molecules, forming layers parallel to the crystallographic *ac* plane (Fig. 2; Table S1, Supporting information). The binuclear units of **1** are held together also by the C–H···Cl hydrogen bonds summarized in Table S2, Supporting information. The hydrogen bonds C(3)–H(3)···Cl(1)^{ii} [(ii) = –x, 1 – y, –z] and C(2)–H(2)···Cl(1)^{iv} [(iv) = x, –1 + y, z] arrange the molecular layers in a three-dimensional crystal architecture.
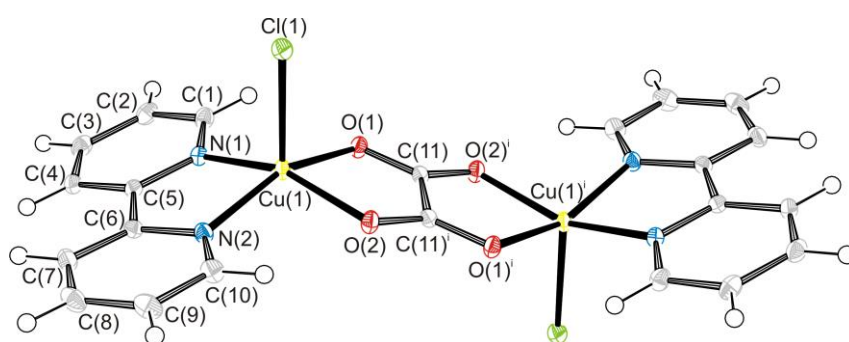
Fig. 1. Molecular structure of the binuclear [Cu(bpy)Cl(μ-C$_2$O$_4$)Cu(bpy)Cl] unit of **1** with the atom-numbering scheme. Displacement ellipsoids are drawn at the 50% probability level. Symmetry operator: (i) 1 – x, 1 – y, 1 – z.

Table 2
Selected bond lengths (Å) and angles (°) for compound **1**.

|			
Cu(1)−N(1)	1.9735(14)	Cl(1)−Cu(1)−O(2)	100.04(4)
Cu(1)−N(2)	1.9951(14)	O(1)−Cu(1)−O(2)	83.64(5)
Cu(1)−O(1)	2.0162(13)	O(1)−Cu(1)−N(1)	93.15(5)
Cu(1)−O(2)	1.9987(12)	O(1)−Cu(1)−N(2)	155.95(5)
Cu(1)−Cl(1)	2.3869(10)	O(2)−Cu(1)−N(1)	158.18(5)
Cl(1)−Cu(1)−N(1)	101.77(5)	O(2)–Cu(1)−N(2)	92.55(5)
Cl(1)−Cu(1)−N(2)	104.29(5)	N(1)−Cu(1)−N(2)	81.61(6)
Cl(1)−Cu(1)−O(1)	99.76(4)		
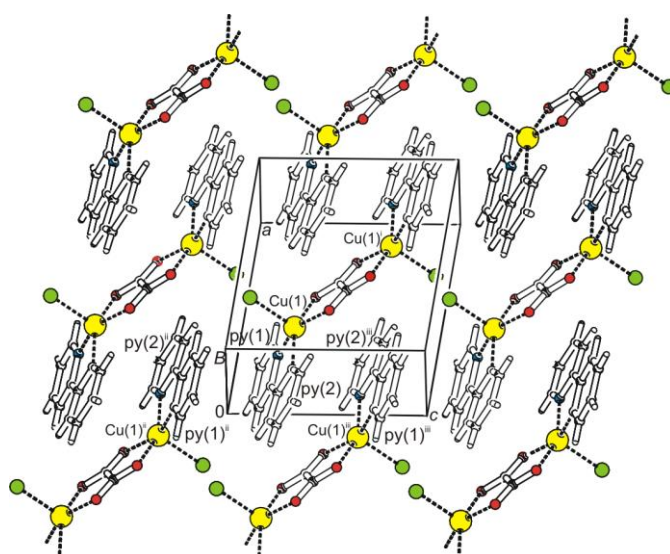
Fig. 2. The layer parallel to the *ac* plane in **1** generated by the $\pi\cdots\pi$ intermolecular interactions between aromatic rings of the bipyridine ligands [symmetry operators: (*i*) $1 - x$, $1 - y$, $1 - z$; (*ii*) $-x$, $1 - y$, $-z$; (*iii*) $-x$, $1 - y$, $1 - z$].

3.3. Crystal structure of 2

Compound **2** is isostructural to **1** and, as other measurements also demonstrated (see *Synthesis and characterization*, *Magnetization* and *EPR studies*), it is a cocrystallized system consisting of three types of mutually analogous binuclear species: [Cu(bpy)Cl(μ-C$_2$O$_4$)Cu(bpy)Cl] (**CuCu**; the same unit as in **1**), [Cu(bpy)Cl(μ-C$_2$O$_4$)Zn(bpy)Cl] (**CuZn**) and [Zn(bpy)Cl(μ-C$_2$O$_4$)Zn(bpy)Cl] (**ZnZn**). Because of the impossibility of differentiating Cu from Zn through the refinement methods, based on the elemental analysis and the magnetic measurements findings (see below), the crystal structure of **2** was modelled as substitutionally disordered with the three types of binuclear units randomly distributed throughout the crystalline lattice in the molar ratio of 1 : 2 : 1 (for details see Experimental, Single-crystal X-

ray study). Selected geometric parameters of the entities found in **2** are given in Table 3. The bond lengths and angles including the Cu atom are very similar to those in **1**. The Zn−Cl bond [2.257(8) Å] in **2** is shorter than the Cu−Cl bond in **1** and **2** [2.3869(10) and 2.395(8) Å, respectively; Tables 2 and 3]. The Zn−O and Zn−N bond lengths are almost equal, with the average values of 2.055 and 2.0545 Å, respectively. Comparable values for the Zn−O bonds are found in the oxalate-bridged compounds $[Zn_3(4,4'-bpy)_4(\mu-C_2O_4)_3]_n$ (2.074 Å in average) and $[Zn(4,4'-bpy)(\mu-C_2O_4)]_n$ [2.083(3) Å] (4,4'-bpy = 4,4'-bipyridine) [33]. However, the Zn−N bonds in **2** are noticeably shorter than the corresponding bonds found in similar zinc(II) species, including the two known 2,2'-bipyridine oxalate complexes, $[Zn(bpy)_2(C_2O_4)]\cdot5H_2O$ (2.1984 Å in average) [34] and $[\{Zn(bpy)_2\}_2(\mu-C_2O_4)][Zn(bpy)_2(\mu-C_2O_4)NbO(C_2O_4)_2]_2\cdot0.5bpy\cdot7H_2O$ (2.1319 Å in average) [30d]. The Cu and Zn atoms are 0.369(5) Å and 0.602(5) Å, respectively, out of the pyramidal basal plane (N_2O_2). The intermetal distances across the bridging oxalate group amount 5.229(5) Å (in **CuCu**), 5.284(5) Å (in **CuZn**) and 5.349(5) Å (in **ZnZn**).
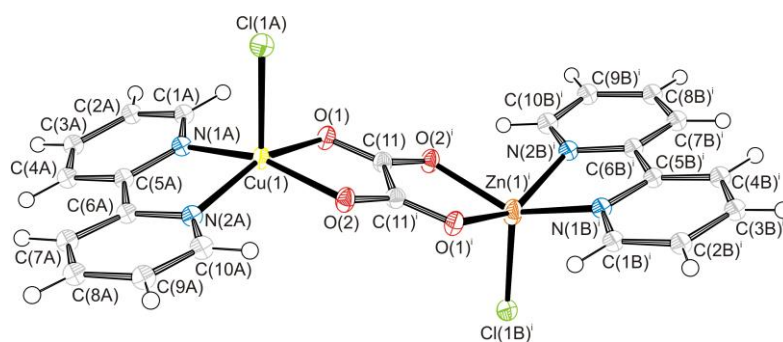
Fig. 3. Molecular structure of the (hetero)binuclear $[Cu(bpy)Cl(\mu-C_2O_4)Zn(bpy)Cl]$ (**CuZn**) unit of **2** with the atom-numbering scheme. The homobinuclear **CuCu** and **ZnZn** entities are also present, but are omitted for clarity. The atoms denoted by 'A' belong to the ligands bound to Cu, and those denoted by 'B' to the ligands bound to Zn. Displacement ellipsoids are drawn at the 50% probability level. Symmetry operator: (*i*) $1 - x$, $1 - y$, $1 - z$.

3.4. Infrared Study

The IR spectra of **1** and **2** show characteristic absorption bands of bridging oxalate groups, coordinated bipyridine ligands and the metal–chlorine bonds. The absorption bands corresponding to the bridging oxalate ligand are located at 1647 cm^{-1} [ν_{as}(CO)], 1351 cm^{-1} [ν_s(CO)] and 796 cm^{-1} [δ(OCO)] in the spectrum of **1** and at 1649 cm^{-1} [ν_{as}(CO)], 1352 cm^{-1} [ν_s(CO)] and 797 cm^{-1} [δ(OCO)] in the spectrum of **2** [19c,35]. The absorption band with a maximum located at 325 cm^{-1} in the spectrum of **1** could be recognized as ν(Cu–Cl) [36]. In

the spectrum of compound **2**, which contains both, the copper–chlorine and the zinc–chlorine bonds, two corresponding ν(M–Cl) absorption band was found, at 325 and 298 cm^{-1}, respectively [36,37]. Other absorption bands in the spectra originate from different vibrations of coordinated 2,2'-bipyridine molecules [35].

Table 3
Selected bond lengths (Å) and angles (°) for compound **2**.

Cu(1)−N(1A)	1.973(8)	Zn(1)−N(1B)	2.052(8)
Cu(1)−N(2A)	2.005(8)	Zn(1)−N(2B)	2.057(8)
Cu(1)−O(1)	2.030(6)	Zn(1)−O(1)	2.046(6)
Cu(1)−O(2)	1.991(6)	Zn(1)−O(2)	2.064(6)
Cu(1)–Cl(1A)	2.395(8)	Zn(1)–Cl(1A)	2.257(8)
Cl(1A)−Cu(1)−N(1A)	99.7(4)	Cl(1B)−Zn(1)−N(1B)	109.0(4)
Cl(1A)−Cu(1)−N(2A)	104.7(4)	Cl(1B)−Zn(1)−N(2B)	108.4(4)
Cl(1A)−Cu(1)−O(1)	99.1(3)	Cl(1B)−Zn(1)−O(1)	105.1(4)
Cl(1A)−Cu(1)−O(2)	98.9(3)	Cl(1B)−Zn(1)−O(2)	105.7(4)
O(1)−Cu(1)−O(2)	83.4(2)	O(1)−Zn(1)−O(2)	81.2(2)
O(1)−Cu(1)−N(1A)	92.8(3)	O(1)−Zn(1)−N(1B)	91.7(3)
O(1)−Cu(1)−N(2A)	156.2(4)	O(1)−Zn(1)−N(2B)	146.5(4)
O(2)−Cu(1)−N(1A)	161.3(4)	O(2)−Zn(1)−N(1B)	145.3(4)
O(2)–Cu(1)−N(2A)	94.4(3)	O(2)−Zn(1)−N(2B)	88.7(3)
N(1A)−Cu(1)−N(2A)	81.6(3)	N(1B)−Zn(1)−N(2B)	78.6(3)

3.5. Magnetization study

The results of magnetic measurements for compounds **1** and **2** are shown in Figs. 4 and 5, in the term of temperature dependence of molar susceptibility, χ. In the low temperature region (< 25 K) χ follows the Curie's $M \sim T^{-1}$ law for both **1** and **2** (Figs. 4 and 5), but the two compounds differ in the values of susceptibilities obtained. Notably higher values of χ for **2** than those for **1**, imply that compound **2** contains a significantly larger amount of paramagnetic centres per mole than compound **1**. This finding is in line with the expectations that are based on the composition of the compounds, since heterometallic species **2**, containing the diamagnetic Zn ions, allows more paramagnetic pairs to be formed. Additionally, for compound **1**, a broad minimum of susceptibility can be observed between 60 K and 100 K, followed by a rise of susceptibility with the increase of temperature; such a pattern could be assigned to the thermal decoupling of antiferromagnetic dimers. In the same region of the χ *vs T* curve for compound **2**, there is not emphasized any minimum of susceptibility, and this should indicate a smaller amount of antiferromagnetic pairs in this compound as compared with compound **1**. In view of the differences observed between **1** and **2**, a consistent analysis of susceptibility for the two compounds had to be made in order to reveal the magnetic behaviour of these structurally similar systems. On that account, several different methods of analysis were employed independently.
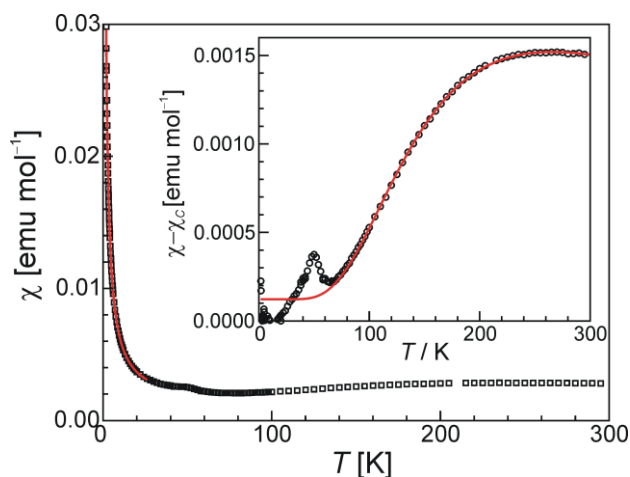
Fig. 4 The temperature dependence of molar susceptibility χ (open squares) with the Curie fit $\chi_C(T)$ for the low-temperature region (solid line) for compound **1**. Inset: The temperature dependence of $\chi - \chi_C$ (open circles) with the Bleaney-Bowers fit (solid line).

As already mentioned, the low-temperature data (< 25 K) for both compounds could be described very well by the Curie's law, $\chi = C/T$. When the Curie-Weiss law, $\chi = C/(T - \theta)$, was used instead, the C constant remained unchanged and the θ parameter amounted between 10 mK and 20 mK. Therefore, in the further analysis procedure, the corresponding Curie's part of susceptibility (χ_C) was subtracted from the total value of χ, in the whole range of temperatures. The remaining part, $\chi - \chi_C$, begins to rise with temperature increasing above 70 K, attaining a maximum value at about 250 K, and decreasing slightly above this temperature, as presented in the insets of Figs. 4 and 5. The observed behaviour for **1** and **2** above 70 K should correspond to the excitation from the singlet to the triplet state of the exchange-coupled spin pairs, in accord with the structure analysis of the compounds. Indeed, the difference $\chi - \chi_C$ can be described very successfully by the Bleaney-Bowers term based on the mutually non-interacting antiferromagnetically coupled spin pairs [38]. Therefore, the temperature dependence of the susceptibility as a whole for **1** and **2**, can be explained by the superposition of two spins $S = 1/2$ from the exchange-coupled oxalate-bridged copper(II) ions and the paramagnetic units containing single copper(II) ions.

The irregular behaviour observed between 40 and 50 K was assumed to come out from the oxygen present in the sample ampoule. This disturbance became pronounced because the Curie's contribution decreased considerably and the triplet excitation did not arise sufficiently at this temperature. The data obtained in this temperature range were excluded from the fitting procedures. Fortunately, this range is just between the two relevant regions and does not influence the analysis of either of them.
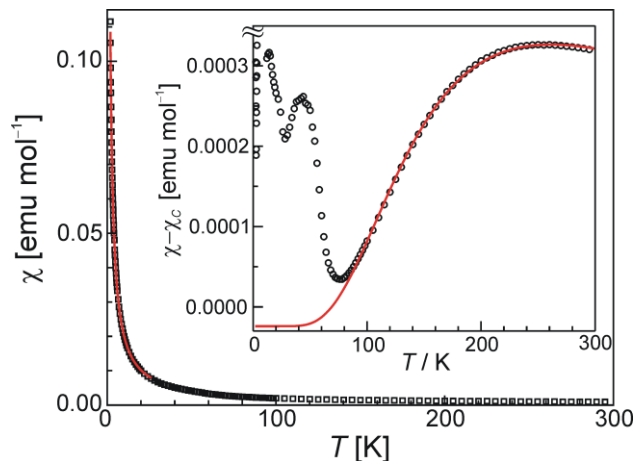
Fig. 5. The temperature dependence of molar susceptibility χ (open squares) with the Curie fit $\chi_C(T)$ for the low-temperature region (solid line) for compound **2**. Inset: The temperature dependence of $\chi - \chi_C$ (open circles) with the Bleaney-Bowers fit (solid line).

The quantitative consideration of the Curie and Bleaney- Bowers [38] terms enables one to determine the number of paramagnetic entities and antiferromagnetically coupled pairs in the examined compounds. The susceptibility contribution is directly proportional to the molar amount w of the corresponding units in the sample. Starting with compound **2** which contains both Cu and Zn metal ions and shows two kinds of magnetic behaviour (paramagnetic at low temperatures and the singlet to triplet transition of the magnetic dimers at higher temperatures), it was reasonable to presume that this compound includes at least two different types of binuclear magnetic entities: **CuZn** ([Cu(bpy)Cl(μ-C_2O_4)Zn(bpy)Cl]) and **CuCu** ([Cu(bpy)Cl(μ-C_2O_4)Cu(bpy)Cl]). The spin 1/2 from the copper(II) centre gives a paramagnetic feature to the **CuZn** entity. Therefore, the nonlinear fit procedure of the Curie's dependence:

$$\chi_{CuZn} = w_{CuZn} \frac{N_A \mu_B^2 g^2}{4k_B T} \tag{1}$$

for which N_A, μ_B, g, k_B and T have their usual meanings, to the lower temperature part (below 25 K) of the measured data gives the molar proportion w_{CuZn} of the **CuZn** pairs in the sample. For the g factor, $\langle g^2 \rangle = 4.62$ as obtained from the EPR measurements (see EPR study) was used. For the **CuCu** entities the susceptibility is given by the Bleaney-Bowers expression [38]:

$$\chi_{CuCu} = w_{CuCu} \frac{2N_A\mu_B^2 g^2}{k_B T\left(3 + e^{-J/k_B T}\right)} \tag{2}$$

for which J is the exchange interaction energy between copper(II) spins, defined by the spin Hamiltonian $\mathbf{H} = -J\mathbf{S_1 \cdot S_2}$, with $S_1 = S_2 = 1/2$. After the **CuZn** Curie contribution [relation (1)] was subtracted, the above expression (2) was fitted to the experimental data above 80 K and extrapolated to the whole temperature range; this procedure gave the molar proportion w_{CuCu} of the **CuCu** pairs in the sample. Based on the calculated w_{CuCu} and w_{CuZn} values, the amount of the **ZnZn** entities could be derived as $[1 - (w_{CuCu} + w_{CuZn})]$. The contribution of the **ZnZn** pairs is diamagnetic and thus mixed with diamagnetic contributions of all other atoms; therefore, the diamagnetic contribution calculated in this case could not provide the precise amount of the **ZnZn** pairs. This procedure resulted with the following values: $w_{CuZn} = 0.46(1)$, $w_{CuCu} = 0.22(1)$ and $w_{ZnZn} = 0.32(1)$ for compound **2**. Compound **1** contains only the Cu metal ions; consequently, only the [Cu(bpy)Cl(μ-C$_2$O$_4$)Cu(bpy)Cl] binuclear entities could exist in this species. Nevertheless, the low-temperature susceptibility behaviour shows that there are paramagnetic ions present in the sample. Fitting the Curie dependence to the experimental data reveals that 5.9% of the copper(II) ions in the sample of **1** are not coupled into dimers. The presence of the non-coupled copper(II) impurities (evidenced at the lowest temperatures through a slight increase in χ) is a phenomenon common for this type of antiferromagnetic species [39].

The coupling of two copper(II) ions through the oxalate-bridge makes a strong exchange interaction, with $J = -295(2)$ and $-294(2)$ cm^{-1} for **1** and **2**, respectively. It is known that in the complexes with two square-pyramidal copper(II) centres and an entirely planar [LCu(μ-C$_2$O$_4$)CuL] array, the $d_{x^2-y^2}$ magnetic orbital of copper(II) should be ideally directed towards the oxalate σ orbitals, and the antiferromagnetic interaction would be maximized (J from -280 to -400 cm^{-1}) [32a]. Several structural parameters in oxalate-bridged binuclear copper(II) complexes, such as the Cu$\cdots$Cu separation across the bridging oxalate ($d_{Cu\cdots Cu}$), the dihedral angle between the plane of the oxalate ligand and the mean basal plane (φ), or the amount of the out-of-plane displacement of the copper(II) ions (h_{Cu}), influence the strength of antiferromagnetic interaction within the designated range [7e]. The values of these parameters for compounds **1** and **2** are mostly somewhat higher than those for similar oxalate-bridged copper(II) species (Table 4); this finding could account for noticeably weaker

antiferromagnetic couplings in **1** and **2** than found in the related compounds (Table 4) [7c,7d].

Table 4
Selected magneto-structural parameters for oxalate-bridged copper(II) complexes of the type $[LCu(\mu\text{-}C_2O_4)CuL]X_2$.

L [a]	X	Donor set	φ [b]	h_{Cu} [c]	$d_{Cu\cdots Cu^i}$ [d]	J [e]	Ref.
bpy	NO_3	O_2N_2/O_2	4.6	0.11	5.143	-382	31a
bpy	NO_3	O_2N_2/O	3.2	0.16	5.154(1)	-386	19a,19c
bpy	ClO_4	O_2N_2/O	12.0	0.18	5.150(1)	-376	19c
bpy	BF_4	O_2N_2/O	10.4	0.16	5.144(1)	-378	19c
phen	NO_3	O_2N_2/O	16.9	0.27	5.158(1)	-330	7b
tmen	ClO_4	O_2N_2/O	8.4	0.18	5.147/5.	$-$	6a, 7a
dpp	NO_3	O_2N_2/O_2	7.3	0.16	5.171(1)	-312	7c
Pz_2CP	Cl	O_2N_2/Cl	20.3	0.39	5.212	-364	7d
Pz_2CP	NO_3	O_2N_2/O	18.7	0.35	5.161	-344	7d
Pz_2CP	ClO_4	O_2N_2/O	2.6	0.36	f	-424	7d
Pz^{3m}_2	NO_3	O_2N_2/O	23.6	0.34	5.178	-378	7d
bpy	Cl	O_2N_2/Cl	16.9	0.40	5.227(2)	-295	this

[a] Abbreviations: bpy = 2,2-bipyridine; phen = 1,10-phenathroline; tmen = N,N,N',N'-tetramethylethylenediamine*;* dpp = 2,3-bis(2-pyridyl)pyrazine; Pz_2CPh_2 = diphenyldipyrazolylmethane; $Pz^{3m}_2CPh_2$ = diphenylbis(3-methylpyrazolyl)methane. [b] Dihedral angle (°) between mean oxalate and equatorial planes. [c] Distance of the copper atom from basal plane (Å). [d] Metal–metal separation across the oxalate bridge in symmetric binuclear copper(II) compounds (Å). [e] Magnetic coupling in cm^{-1}. [f] Not reported.

3.6. EPR study

The EPR spectra of compounds **1** and **2** at three different temperatures (T = 5, 100 and 295 K) are shown in Figs. 6 and 7, respectively. The intensities of the spectra at 100 and 295 K are given multiplied by some constant values, as indicated in the Figs. In all spectra, a signal of low intensity, originating from the EPR cavity, appears at low fields (around 175 mT). All spectral simulations were carried out by the XSophe software [40]. The spectrum of compound **1**, recorded at the lowest measured temperature (T = 5 K), exhibits four hyperfine lines as anticipated for a copper(II) centre. The intensity of the spectrum indicates a low concentration of these copper(II) centres (~10^{21} centres/mol); the spectrum is therefore assigned to the uncoupled copper(II) ions (paramagnetic impurities), the presence of which was confirmed also by the magnetization measurements (5.9%). No additional contribution that would originate from the binuclear oxalate-bridged [Cu(bpy)Cl(μ-C_2O_4)Cu(bpy)Cl] units of **1**, was detected in the spectrum. This is in accord with the existence of the

antiferromagnetic ground state ($S = 0$) and a strong exchange interaction ($J = -295(2)$ cm^{-1}, as observed in the magnetization experiment). Although the exact nature and structure of the impurities are not entirely known, assuming the same environment around the copper(II) centres in the impurities as in the dimers, the spin-Hamiltonian

$$\mathbf{H} = \mu_B \mathbf{B} \cdot \mathbf{g} \cdot \mathbf{S} + \mathbf{S} \cdot \mathbf{A} \cdot \mathbf{I} \qquad\qquad (3)$$

was employed to describe these centres more quantitatively [41]. In relation (3), $\mathbf{g}$ represents g tensor, $\mathbf{A}$ is hyperfine splitting tensor, $\mathbf{B}$ is magnetic field, $\mathbf{S}$ is electron spin operator whereas $\mathbf{I}$ is nuclear spin operator ($S = 1/2$, $I = 3/2$). The spectrum was simulated assuming an axial symmetry of $\mathbf{g}$ and $\mathbf{A}$ tensors. The simulated spectrum, at $T = 5$ K, shown in Fig. 6, was obtained using the following parameters: $g_x = g_y = 2.081$, $g_z = 2.280$, $A_x = A_y = 0$ and $A_z = 154 \times 10^{-4}$ cm^{-1}, with an effective linewidth of 3.5 mT. The obtained values $g_\parallel > g_\perp$ point out that the unpaired electron is located in the $d_{x^2-y^2}$ orbital, in accord with the square-pyramidal environment around the copper(II) centres [42]. With a rise of temperature, the number of binuclear copper(II) units of compound **1**, that were excited from the ground spin-singlet state ($S = 0$) to the higher spin-triplet state ($S = 1$) grew up [39]. The spins $S = 1$ became magnetically diluted centres in the mainly diamagnetic lattice ($S = 0$). The presence of a fine interaction (zero-field splitting) of these binuclear [Cu(bpy)Cl(μ-C$_2$O$_4$)Cu(bpy)Cl] entities could be observed as a deviation of the spectrum recorded at $T = 100$ K from the simulated spectrum that was obtained by the same spin-Hamiltonian parameters as the spectrum simulated at $T = 5$ K. At higher temperatures, the majority of molecules are in the spin-triplet ($S = 1$) state. Because of the inter-dimer interactions, the observed spectra, due to an expected increase of the linewidth, no longer exhibit hyperfine and fine structure. Indeed, this effect can be observed as a broad spectrum detected at $T = 295$ K. The spectrum was simulated with the same parameters as previously, taking into account that the linewidth of the broader line is one order of magnitude greater than the linewidth of the line at low temperatures.
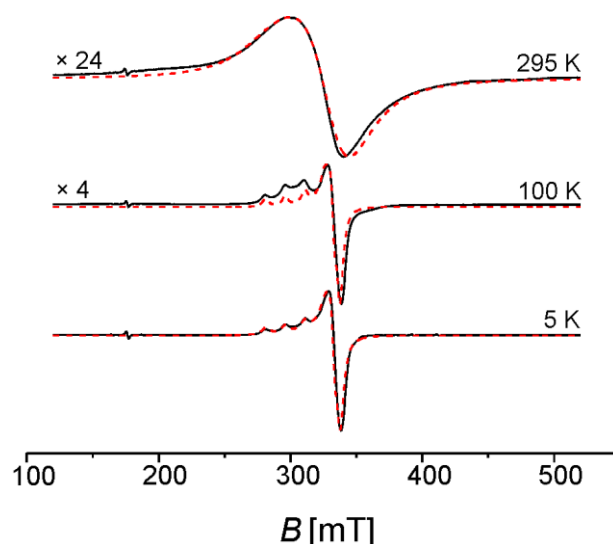
Fig. 6. The experimental (solid lines) and simulated (dashed lines) X-band EPR spectra of a powdered sample of **1** at the indicated temperatures.

As for compound **2**, a hyperfine structure of the copper(II) centres could be observed in all recorded EPR spectra (Fig. 7). At $T = 5$ K, the spectrum of **2** shows a much higher intensity as compared with the spectrum of **1**, thus indicating that this spectrum originates from the copper(II) centres in the **CuZn** pairs (the number of copper(II) centres/mol present in compound **2** is two orders of magnitude higher than that in compound **1**). The spectra of compound **2** could be well simulated at all temperatures measured, using the same spin-Hamiltonian parameters as for **1**, and taking into consideration only the line broadening due to the change of temperature. This reveals the same environments around copper(II) centres in the **CuZn** pairs in **2** as those in the paramagnetic impurities in **1**. With an increase of temperature, the number of the **CuCu** pairs in the spin-triplet state ($S = 1$) increased, the same as in compound **1**, but this gives rather a small contribution to the total spectrum of **2**, which is mainly due to the paramagnetic **CuZn** pairs. This is in agreement with the magnetization measurements results that the total number of the **CuCu** pairs is about two times lower than the number of the dominant paramagnetic **CuZn** pairs.
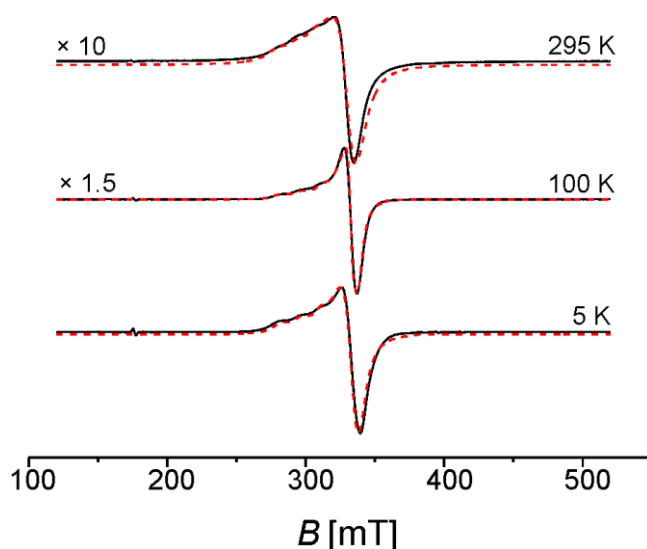
Fig. 7. The experimental (solid lines) and simulated (dashed lines) X-band EPR spectra of a powdered sample of **2** at the indicated temperatures.

4. Conclusions

Two new oxalate-bridged compounds, $[\{Cu(bpy)Cl\}_2(\mu\text{-}C_2O_4)]$ (**1**) and $[CuZn\{(bpy)Cl\}_2(\mu\text{-}C_2O_4)]$ (**2**) (bpy = 2,2'-bipyridine) resulted from a rather unusual synthetic procedure. It turned out that the presence of a niobium(IV) intermediate in the reaction mixture was essential for the incorporation of Zn into the unique system of **2**, which is generally the first, fully characterized species with the $Cu(\mu\text{-}C_2O_4)Zn$ bridge. The crystal structure of compound **1** consists of the centrosymmetric binuclear entities $[Cu(bpy)Cl(\mu\text{-}C_2O_4)Cu(bpy)Cl]$, with a square-pyramidal N_2O_2Cl environment around the metal centres. A particularly interesting feature of compound **2** is the fact that it comprises three types of binuclear entities: $[Cu(bpy)Cl(\mu\text{-}C_2O_4)Cu(bpy)Cl]$ (**CuCu**; the same as in **1**), $[Cu(bpy)Cl(\mu\text{-}C_2O_4)Zn(bpy)Cl]$ (**CuZn**) and $[Zn(bpy)Cl(\mu\text{-}C_2O_4)Zn(bpy)Cl]$ (**ZnZn**), randomly distributed throughout the crystal in the molar ratio close to 1 : 2 : 1. Such a rarely observed crystal structure was resolved through a comprehensive approach, taking into account all other measurements carried out in the research. The binuclear entities in the crystal packing of both **1** and **2** are linked by the intermolecular $\pi\cdots\pi$ stacking interactions into the layers, whereas the additional weak $C–H\cdots Cl$ hydrogen bonds lead to the overall three-dimensional crystal architecture.

The magnetization measurements, supported by the EPR study, revealed the existence of a strong antiferromagnetic interaction between the copper(II) ions through the oxalate bridge for both compounds ($J = –295(2)$ and $–294(2)$ cm^{-1} for **1** and **2**, respectively). Also, molar

proportions of the individual dimeric components present in the samples were determined and found to be in accordance with the overall data.

Acknowledgements

Appendix A. Supplementary data

CCDC 671249 and 671250 contains the supplementary crystallographic data for compounds **1** and **2**. These data can be obtained free of charge via http://www.ccdc.cam.ac.uk/conts/retrieving.html, or from the Cambridge Crystallographic Data Centre, 12 Union Road, Cambridge CB2 1EZ, UK; fax: (+44) 1223-336-033; or e-mail: deposit@ccdc.cam.ac.uk. Supplementary data associated with this article can be found, in the online version, at http://dx.doi.org/

References

[1]   (a) G. Marinescu, M. Andruh, F. Lloret, M. Julve, Coord. Chem. Rev. 255 (2011) 161–185;
(b) C. N. R. Rao, S. Natarajan, R. Vaidhyanathan, Angew. Chem. Int. Ed. 43 (2004) 1466–1496;
(c) F. H. Allen, Acta Crystallogr., Sect. B 58 (2002) 380–388;
(d) M. Hernández-Molina, P. A. Lorenzo-Luis, C. Ruiz-Pérez, CrystEngComm 16 (2001) 1–4;
(e) A. Świtlicka-Olszewska, B. Machura, J. Mroziński, B. Kalińska, R. Kruszynski, M. Penkala, New J. Chem. 38 (2014) 1611–1626.
[2]   (a) X. Chen, S. Han, R. Wang, CrystEngComm 14 (2012) 6400–6403;
(b) C. Borel, K. Larsson, M. Håkansson, B. E. Olsson, A. D. Bond, L. Öhrström, Cryst. Growth Des. 9 (2009) 2821–2827;
(c) S. R. Batten, J. Solid State Chem. 178 (2005) 2475–2479;
(d) J. Y. Lu, Coord. Chem. Rev. 246 (2003) 327–347;
(e) S. Decurtins, R. Pellaux, G. Antorrena, F. Palacio, Coord. Chem. Rev. 190–192 (1999) 841–854.
[3]   (a) O. Khan, Molecular Magnetism, VCH, Weinheim, Germany, 1993, and references therein;
(b) W. Linert, M. Verdaguer, (Eds.) Molecular Magnets – Recent Highlights, Springer-Verlag, Wien, 2003;
(c) X.-Y. Wang, C. Avendaño, K. R. Dunbar, Chem. Soc. Rev. 40 (2011) 3213–3238;
(d) M. Clemente-León, E. Coronado, C. Martí-Gastaldo, F. M. Romero, Chem. Soc. Rev. 40 (2011) 473–497.

[4]   (a) T. Steiner, Angew. Chem. Int. Ed. 41 (2002) 48–76;
       (b) C. Janiak, J. Chem. Soc., Dalton Trans. (2000) 3885–3896.
[5]   (a) K. D. Karlin, J. Zubieta, Copper Coordination Chemistry, Adenine Press, New York, 1983;
       (b) E. I. Soloman, D. W. Randall, T. Glaser, Coord. Chem. Rev. 200 (2000) 595–632;
       (c) P. Comba, R. Remenyi, Coord. Chem. Rev. 238 (2003) 9–20.
[6]   (*a*) M. Julve, M. Verdaguer, O. Kahn, A. Gleizes, M. Philoche-Levisalles, Inorg. Chem. 22 (1983) 368–370;
       (b) Y. Akhriff, J. Server-Carrió, A. Sancho, J. García-Lozano, E. Escrivá, J. V. Folgado, L. Soto, Inorg. Chem. 38 (1999) 1174–1185;
       (c) J. Glerup, P. A. Goodson, D. J. Hodgson, K. Michelsen, Inorg. Chem. 34 (1995) 6255–6264;
       (d) X.-D. Zhang, Z. Zhao, J.-Y. Sun, Y.-C. Ma, M.-L. Zhu, Acta Crystallogr., Sect. E 61 (2005) m2643–m2645;
       (e) S. Youngme, A. Cheansirisomboon, C. Danvirutai, N. Chaichit, C. Pakawatchai, G. A. van Albada, J. Reedijk, Inorg. Chem. Commun. 9 (2006) 973–977;
       (f) M. Wang, B. Hu, X.-T. Deng, C.-G. Wang, Acta Crystallogr., Sect. E 63 (2007) m710–m711;
       (g) A. Recio, J. Server-Carrió, E. Escrivá, R. Acerete, J. García-Lozano, A. Sancho, L. Soto, Cryst. Growth Des. 8 (2008) 4075–4082.
[7]   (a) M. Julve, M. Verdaguer, A. Gleizes, M. Philoche-Levisalles, O. Kahn, Inorg. Chem. 23 (1984) 3808–3818;
       (b) A. Bencini, A. C. Fabretti, C. Zanchini, P. Zannini, Inorg. Chem. 26 (1987) 1445–1449;
       (c) J. Carranza, H. Grove, J. Sletten, F. Lloret, M. Julve, P. E. Kruger, C. Eller, D. P. Rillema, Eur. J. Inorg. Chem. (2004) 4836–4848;
       (d) J. L. Shaw, G. T. Yee, G. Wang, D. E. Benson, C. Gokdemir, C. J. Ziegler, Inorg. Chem. 44 (2005) 5060–5067;
       (e) M. J. Belousoff, B. Graham, B. Moubaraki, K. S. Murray, L. Spiccia, Eur. J. Inorg. Chem. (2006) 4872–4878;
       (f) G.-L. Zhang, Y.-T. Li and Z.-Y. Wu, Acta Crystallogr., Sect. E 62 (2006) m1175–m1177;
       (g) S. C. Manna, J. Ribas, E. Zangrando, N. R. Chaudhuri, Inorg. Chim. Acta 360 (2007) 2589–2597.
[8]   (a) X. Wang, C. Qin, E. Wang, Y. Li, N. Hao, C. Hu, L. Xu, Inorg. Chem. 43 (2004) 1850–1856;
       (b) L. Xu, G.-C. Guo, B. Liu, M.-S. Wang, J.-S. Huang, Inorg. Chem. Commun. 7 (2004)1145–1149;
       (c) E. J. O'Neil, B. D. Smith, Coord. Chem. Rev. 250 (2006) 3068–3080;
       (d) Y.-S. Song, B. Yan, Z.-X. Chen, Appl. Organomet. Chem. 20 (2006) 44–50;
       (e) S. Miyatsu, M. Kofu, A. Nagoe, T. Yamada, M. Sadakiyo, T. Yamada, H. Kitagawa, M. Tyagi, V. G. Sakai, O. Yamamuro, Phys. Chem. Chem. Phys. 16 (2014) 17295–17304.
[9]   (a) L.-N. Zhu, L. Z. Zhang, W.-Z. Wang, D.-Z. Liao, P. Cheng, Z.-H. Jiang, S.-P. Yan, Inorg. Chem. Commun. 5 (2002) 1017–1021;
       (b) L. Wen, Y. Li, D. Dang, Z. Tian, Z. Ni, Q. J. Meng, Solid State Chem. 178 (2005) 3336–3341;
       (c) R. Fu, S. Xiang, S. Hu, L. Wang, Y. Li, X. Huang, X. Wu, Chem. Commun. (2005) 5292–5294;

(d) X. Liu, X. Mu, H. Xia, L. Ye, W. Gao, H. Wang, Y. Mu, Eur. J. Inorg. Chem. (2006) 4317–4323;

(e) J. He, Y.-G. Yin, X.-C. Huang, D. Li, Inorg. Chem. Commun. 9 (2006) 205–207;

(f) G. Tian, G. Zhu, Q. Fang, X. Guo, M. Xue, J. Sun, S. Qiu, J. Mol. Struct. 787 (2006) 45–49.

[10]   (a) D. S. Auld, Biometals 14 (2001) 271–313;

(b) L. M. Berreau, Eur. J. Inorg. Chem. (2006) 273–283;

(c) A. Tamilselvi, M. Nethaji, G. Mugesh, Chem. Eur. J. 12 (2006) 7797–7806;

(d) E. Jaime and J. Weston, Eur. J. Inorg. Chem. 2006, 793–801.

[11]   (a) S. Albedyhl, D. Schnieders, A. Jancsó, T. Gajda, B. Krebs, Eur. J. Inorg. Chem. (2002) 1400–1409;

(b) D. Ghosh, N. Kundu, G. Maity, K.-Y. Choi, A. Caneschi, A. Endo, M. Chaudhury, Inorg. Chem. 43 (2004) 6015–6023;

(c) B. Bauer-Siebenlist, F. Meyer, E. Farkas, D. Vidovic, S. Dechert, Chem. Eur. J. 11 (2005) 4349–4360;

(d) B. Bauer-Siebenlist, S. Dechert, F. Meyer, Chem. Eur. J. 11 (2005) 5343–5352;

(e) J. W. Chen, X. Y. Wang, Y. G. Zhu, J. Lin, X. L. Yang, Y. Z. Li, Y. Lu, Z. J. Guo, Inorg. Chem. 44 (2005) 3422–3430.

[12]   (a) R. N. Patel, K. B. Pandeya, J. Inorg. Biochem. 72 (1998) 109–114;

(b) R. N. Patel, S. Kumar, K. B. Pandeya, Spectrochim. Acta Part A 56 (2000) 2791–2797;

(c) R. N. Patel, Spectrochim. Acta Part A 59 (2003)713–721.

[13]   (a) R. N. Patel, N. Singh, R. P. Shrivastava, S. Kumar, J. Mol. Liq. 89 (2000) 207–221;

(b) R. N. Patel, S. Kumar, K. B. Pandeya, P. V. Khadikar, Spectrochim. Acta Part A 58 (2002) 2961–2969;

(c) R. N. Patel, S. Kumar, K. B. Pandeya, J. Inorg. Biochem. 89 (2002) 61–68;

(d) R. N. Patel, J. Mol. Liq. 122 (2005) 104–109;

(e) R. N. Patel, N. Singh, K. K. Shukla and U. K. Chauhan, Spectrochim. Acta Part A 61 (2005) 287–297.

[14]   (a) N. Singh, K. K. Shukla, R. N. Patel, U. K. Chauhan, R. P. Shrivastava, Spectrochim. Acta Part A 59 (2003) 3111–3122;

(b) I. Szilágyi, G. Nagy, K. Hernandi, I. Labádi, I. Pálinkó, J. Mol. Struct. TEOCHEM 666/667 (2003) 451–453;

(c) L. M. Mirica, X. Ottenwaelder, D. P. Stack, *Chem. Rev.* 104 (2004) 1013–1045;

(d) R. N. Patel, N. Singh, K. K. Shukla, V. L. N. Gundla, U. K. Chauhan, J. Inorg. Biochem. 99 (2005) 651–663;

(e) I. Szilágyi, I. Labádi, K. Hernandi, I. Pálinkó, N. V. Nagy, L. Korecz, A. Rockenbauer, Z. Kele, T. Kiss, J. Inorg. Biochem. 99 (2005) 1619–1629.

[15]   (a) H. Ohtsu, S. Fukuzumi, Angew. Chem. Int. Ed. 39 (2000) 4537–4539;

(b) H. Ohtsu and S. Fukuzumi, Chem. Eur. J. 7 (2001) 4947–4953;

(c) B. Verdejo, S. Blasco, E. García-España, F. Lloret, P. Gavina, C. Soriano, S. Tatay, H. R. Jiménez, A. Doménech, J. Latorre, Dalton Trans. (2007) 4726–4737.

[16]   (a) J.-L. Pierre, P. Chautemps, S. Refaif, C. Beguin, A. El Marzouki, G. Serratrice, E. Saint-Aman, P. Rey, J. Am. Chem. Soc. 117 (1995) 1965–1973;

(b) H. Ohtsu, Y. Shimazaki, A. Odani, O. Yamauchi, W. Mori, S. Itoh, S. Fukuzumi, J. Am. Chem. Soc. 122 (2000) 5733–5741;

(c) D. Li, S. Li, D. Yang, J. Yu, J. Huang, Y. Li and W. Tang, Inorg. Chem. 42 (2003) 6071–6080;

(d) S.-A. Li, D.-F. Li, D.-X. Yang, Y.-Z. Li, J. Huang, K.-B. Yu, W.-X. Tang, Chem. Commun. (2003) 880–881;

(e) Q. Yuan, K. Cai, Z.-P. Qi, Z.-S. Bai, Z. Su, W.-Y. Sun, J. Inorg. Biochem. 103 (2009) 1156–1161.

[17] R. N. Patel, N. Singh, K. K. Shukla, U. K. Chauhan, S. Chakraborty, J. Niclos-Gutierez, A. Castineiras, J. Inorg. Biochem. 98 (2004) 231–237.

[18] (a) U. Mukhopadhyay, L. Govindasamy, K. Ravikumar, D. Velmurugan, D. Ray, Inorg. Chem. Commun. 1 (1998) 152–154;

(b) Z.-L. You, L.-L. Ni, P. Hou, J.-C. Zhang, C. Wang, J. Coord. Chem. 63 (2010) 515–523.

[19] (a) M. Julve, J. Faus, M. Verdaguer, A. Gleizes, J. Am. Chem. Soc. 106 (1984) 8306–8308;

(b) I. Castro, J. Faus, M. Julve, M. C. Muñoz, W. Diaz, X. Solans, Inorg. Chim. Acta 179 (1991) 59–66;

(c) A. Gleizes, M. Julve, M. Verdaguer, J. A. Real, J. Faus, X. Solans, J. Chem. Soc. Dalton Trans. (1992) 3209–3216;

(d) J. Shi, G.-M. Yang, P. Cheng, D.-Z. Liao, Z.-H. Jiang, G.-L. Wang, Polyhedron 16 (1997) 531–534;

(e) J. Li, J. Sun, P. Chen and X. Wu, Crys. Res. Technol. 30 (1995) 353–358;

(f) S. Reinoso, P. Vitoria, L. San Felices, L. Lezama and J. M. Gutiérrez-Zorrilla, Acta Crystallogr., Sect. E 61 (2005) m1677–m1679;

(g) G.-X. Liu, K. Zhu, H. Chen, R.-Y. Huang, X.-M. Ren, Z. Anorg. Allg. Chem. 635 (2009) 156–164.

[20] (a) A. M. Thomas, G. C. Mandal, S. K. Tiwary, R. K. Rath, A. R. Chakravarty, J. Chem. Soc., Dalton Trans. (2000) 1395–1396;

(b) S. K. Chattopadhyay, S. Seth, T. C. W. Mak, J. Coord. Chem. 55 (2002) 259–270.

[21] F. M. Jaeger, J. A. van Dijk, Z. Anorg. Allg. Chem. 272 (1936) 273–327.

[22] R. C. Clark, J. S. Reid, Acta Crystallogr., Sect. A 51 (1995) 887–897.

[23] CrysAlis PRO, Oxford Diffraction Ltd., Abingdon, U.K., 2007.

[24] L. J. Farrugia, J. Appl. Crystallogr. 32 (1999) 837–838.

[25] G. Sheldrick, Acta Crystallogr., Sect. A 64 (2008) 112–122.

[26] A. L. Spek, J. Appl. Crystallogr. 36 (2003) 7−13.

[27] L. J. Farrugia, J. Appl. Crystallogr. 30 (1997) 565.

[28] (a) W. Fitzgerald, J. Foley, D. McSweeney, N. Ray, D. Sheahnn, S. Tyagi, B. Hathaway, P. O'Brien, J. Chem. Soc., Dalton Trans. (1982) 1117–1121;

(b) H. Oshio, U. Nagashima, Inorg. Chem. 31 (1992) 3295–3301.

[29] B.-L. Ooi, T. Shihabara, G. Sakane, K.-F. Mok, Inorg. Chim. Acta 266 (1997) 103–107.

[30] (a) M. Šestan, B. Perić, G. Giester, P. Planinić, N. Brničević, Struct. Chem. 16 (2005) 409–414;

(b) M. Jurić, B. Perić, N. Brničević, P. Planinić, D. Pajić, K. Zadro, G. Giester, Polyhedron 26 (2007) 659–672;

(c) M. Jurić, B. Perić, N. Brničević, P. Planinić, D. Pajić, K. Zadro, G. Giester, B. Kaitner, Dalton Trans. (2008) 742–754;

(d) M. Jurić, P. Planinić, N. Brničević, D. Matković-Čalogović, J. Mol. Struct. 888 (2008) 266–276;

(e) M. Jurić, J. Popović, A. Šantić, K. Molčanov, N. Brničević, P. Planinić, Inorg. Chem. 52 (2013) 1832−1842;

(f) J. Popović, M. Vrankić, M. Jurić, Cryst. Growth Des. 13 (2013) 2161−2165.

[31] F. A. Cotton, M. P. Diebold, W. J. Roth, Inorg. Chem. 26 (1987) 2889–2893.

[32] (a) O. Castillo, I. Muga, A. Luque, J. M. Gutiérrez-Zorrilla, J. Sertucha, P. Vitoria, P. Román, Polyhedron 18 (1999)1235–1245;
(b) J. Tang; E. Gao, W. Bu, D. Liao, S. Yan, Z. Jiang, G. Wang, J. Mol. Struct. 525 (2000) 271–275;
(c) A. Castiñeiras; S. Balboa, R. Carballo, J. M. González-Pérez, J. Niclós-Gutiérrez, Z. Anorg. Allg. Chem. 633 (2007) 717–723.

[33] (a) J. Y. Lu, M. A. Lawandy, J. Li, T. Yuen, C. L. Lin, Inorg. Chem. 38 (1999) 2695–2704;
(b) N. Hao, E. Shen, Y. Li, E. Wang, C. Hu and L. Xu, J. Mol. Struct. 691 (2004) 273–277.

[34] M. Šestan Jurić, P. Planinić, G. Giester, Acta Crystallogr., Sect. E 62 (2006) m2826–m2829.

[35] K. Nakamoto, Infrared and Raman Spectra of Inorganic and Coordination Compounds, John Wiley, New York, 6th edn, 2009.

[36] M. Singh, V. Aggarwal, U. P. Singh, N. K. Singh, Polyhedron 28 (2009) 195–199.

[37] D. Kovala-Demertzi, P. N. Yadav, J. Wiecek, S. Skoulika, T. Varadinova, M. A. Demertzis, J. Inorg. Biochem. 100 (2006) 1558–1567.

[38] B. Bleaney, K. D. Bowers, Proc. R. Soc. Lond. A 214 (1952) 451–465.

[39] E. A. Buvaylo, V. N. Kokozay, O. Y. Vassilyeva, B. W. Skelton, J. Jezierska, L. C. Brunel, A. Ozarowski, Chem. Commun. 120 (2005) 4976–4978.

[40] G. R. Hanson, K. E. Gates, C. J. Noble, M. Griffin, A. Mitchell, S. Benson, J. Inorg. Biochem. 98 (2004) 903–916.

[41] D. Pathinettam Padiyan, C. Muthukrishnan, R. Murugesan, J. Magn. Magn. Mater. 222 (2000) 251–256.

[42] X.-F. Chen, P. Cheng, X. Liu, B. Zhao, D.-Z. Liao, S.-P. Yan, Z.-H. Jiang, Inorg. Chem. 40 (2001) 2652–2659.